

Regional lightning NO_x sources during the TROCCINOX experiment

C. Mari¹, J. P. Chaboureaux¹, J. P. Pinty¹, J. Duron¹, P. Mascart¹, J. P. Cammas¹, F. Gheusi¹, T. Fehr², H. Schlager², A. Roiger², M. Lichtenstein², and P. Stock²

¹Laboratoire d'Aérodynamique, UMR CNRS/UPS, Toulouse, France

²DLR, Institut fuer Physik der Atmosphaere, Oberpfaffenhofen, Wessling, Germany

Received: 8 February 2006 – Published in Atmos. Chem. Phys. Discuss.: 26 June 2006

Revised: 23 October 2006 – Accepted: 5 December 2006 – Published: 11 December 2006

Abstract. A lightning NO_x (LiNO_x) source has been implemented in the deep convection scheme of the Meso-NH mesoscale model following a mass-flux formalism coherent with the transport and scavenging of gases inside the convective scheme. In this approach the vertical transport of NO inside clouds is calculated by the parameterization of deep convective transport, thus eliminating the need for a priori LiNO_x profiles. Once produced inside the convective column, NO molecules are redistributed by updrafts and downdrafts and detrained in the environment when the conditions are favorable. The model was applied to three particular flights during the Tropical Convection, Cirrus and Nitrogen Oxides (TROCCINOX) campaign over the tropical area around Bauru on 3–4 March 2004. The convective activity during the three flights was investigated using brightness temperature at 10.7 μm observed from GOES-12 satellite. The use of a model-to-satellite approach reveals that the simulation appears rather realistic compared to the observations. The diurnal cycle of the simulated brightness temperature, CAPE, number of IC flashes, NO entrainment flux are in phase, with a succession of three marked peaks at 18:00 UTC (15:00 LT). These simulated peaks precede the observed afternoon one by about three hours. Comparison of the simulated NO_x with observations along the flight tracks show that the model reproduces well the observed NO_x levels when the LiNO_x source is applied. The budget of entrainment, detrainment and LiNO_x convective fluxes shows that the majority of the NO detrained back to the environment comes from lightning source inside the convective columns. Entrainment of NO from the environment and vertical transport from the boundary layer were not significant during the episode. The troposphere is impacted by detrainment fluxes of LiNO_x from 4 km altitude to 16 km with maximum values around 14 km altitude. Detrainment fluxes vary

between 75 kg(N)/s during nighttime to 400 kg(N)/s at the times of maximum convective activity. Extrapolation of the regional LiNO_x source would yield a global LiNO_x production around 5.7 Tg(N)/year which is within the current estimates but should not hide the overestimation of the number of flash rates by the model.

1 Introduction

Ozone is produced in the troposphere by photochemical oxidation of hydrocarbons and CO catalysed by hydrogen oxide radicals (HO_x = OH + HO₂) and nitrogen oxide radicals (NO_x = NO + NO₂). Consequently changes in atmospheric NO_x concentrations can lead to a modification in the rate of ozone production. NO_x is emitted into the atmosphere from various natural and anthropogenic sources, including fossil fuel combustion, biomass burning, aircraft emission and lightning (Brasseur et al., 1996; Bradshaw et al., 2000). Evidences of NO_x production by lightning were given by airborne measurements in and near mature thunderstorms. Observations at different latitudes show that NO_x can be increased considerably (as much as a few ppbv) in the upper troposphere on small spatial scales (Huntrieser et al., 1998; Dye et al., 2000; Huntrieser et al., 2002; Skamarock et al., 2003)

It is still poorly known how much NO_x is produced by the storms and how this production relates to cloud parameters like particle phase, updraft strength, cloud top height, or flash rate, which all would be useful for parameterisations of NO_x-production. Consequently, estimates of the global NO_x production by lightning in thunderstorms still differ by about one order of magnitude, between 1–20 Tg(N)/year (Price et al., 1997; Lee et al., 1997; Huntrieser et al., 1998). This uncertainty can have great implications in terms of NO_x budget, especially in the southern hemisphere where the LiNO_x source dominates in the upper troposphere (Lamarque et al.,

Correspondence to: C. Mari
(celine.mari@aero.obs-mip.fr)

1997; Zhang et al., 2000; Martin et al., 2000; Hauglustaine et al., 2001).

Although the convective clouds and lightning are local processes, the impact of the LiNO_x source is global. The typical lifetime of NO_x increases from a few hours in the planetary boundary layer to a few days in the upper troposphere, where it can take part in the formation of HNO₃, HNO₄ and PAN. While PAN can act as a NO_x reservoir, HNO₃ can efficiently be scavenged. LiNO_x is closely linked with OH radical production and hence can impact on the oxidizing capacity of the troposphere (Labrador et al., 2004). The chemistry within the high NO_x plume originated from lightning, their long-range transport and their potential importance in sustaining background NO_x far from source regions is still a challenge for global and regional model (Crawford et al., 2000; Tie et al., 2001; Brunner et al., 2003; DeCaria et al., 2005).

Recent satellite observations have demonstrated that, on the global scale, lightning activity is highest over tropical continental areas (Christian et al., 2003). The Tropical Convection, Cirrus and Nitrogen Oxides (TROCCINOX) experiment took place over southern Brazil and provided the first measurements of LiNO_x near deep convective clouds over a continental region in the tropics. This paper focuses on particular convective episodes of the TROCCINOX 2004 experiment when LiNO_x production was found in the upper troposphere. The objective is to quantify the amounts of LiNO_x produced in well-characterised cloud formations and scale up the results of the mission to provide regional estimates of lightning NO_x.

2 Model description

The model used in this study is the Meso-NH model. A full description of the model capabilities is available on <http://www.aero.obs-mip.fr/mesonh> (Lafore et al., 1998). One single domain is used with a horizontal grid of 100×100 points at 30 km resolution and 70 levels with grid spacings from 40 m (bottom) up to 600 m (top). The altitude of the model top is at 27 km. The time step is 30 s. The model starts on 2 March at 00:00 UTC and runs for 66 h. The physics of the model includes the prognostic calculation of the turbulence and a convection scheme based on mass-flux calculations (Bechtold et al., 2001). A mixed-phase microphysics and the subgrid cloudiness are available for these simulations. The surface fluxes are provided by the ISBA (Interaction among Soil-Biosphere-Atmosphere) model (Noilhan, 1989) for the natural patches and TEB (Town Energy Balance) model (Masson et al., 2000) for the urbanized patches. The radiation scheme is the ECMWF scheme (Mlawer et al., 1997). The chemistry scheme includes 37 chemical species representative of the O₃-NO_x-VOC chemistry (Crassier et al., 2000). Emissions are from the EDGAR 3.2 1995 database (Olivier et al., 2001a, b). The initial

and large-scale mixing ratios for chemistry and the meteorological initial and boundary conditions are provided by the MOCAGE (MOdele de Chimie Atmospherique de Grande Echelle) model (Josse et al., 2004; Massart et al., 2005).

The deep convection scheme of Meso-NH (Kain and Fritsch, 1990; Bechtold et al., 2001) has been already adapted by Mari et al. (2000) for the transport and the scavenging of soluble gases.

The mass flux formalism applied to the convective transport of a chemical compound \bar{C} , writes :

$$\left. \frac{\partial \bar{C}}{\partial t} \right|_{\text{convection}} = -\frac{1}{\rho A} \frac{\partial(MC)}{\partial z} - \bar{w} \frac{\partial \bar{C}}{\partial z} \quad (1)$$

where A is the grid mesh area, ρ is the air density, M is the mass flux (in kg/s) and \bar{w} is the environmental subsidence to compensate the upward mass flux. C is the mixing ratio of chemical compound in the convective cells. The mass flux term of Eq. (1) is further decomposed into:

$$\frac{\partial(MC)}{\partial z} = \frac{\partial(M^u C^u)}{\partial z} + \frac{\partial(M^d C^d)}{\partial z} \quad (2)$$

where the superscripts u and d refer to the “updrafts” and to the “downdrafts” components, respectively. The different mass flux divergences are expressed as:

$$\frac{\partial}{\partial z}(M^u C^u) = \epsilon^u \bar{C} - \delta^u C^u \quad (3)$$

$$\frac{\partial}{\partial z}(M^d C^d) = \epsilon^d \bar{C} - \delta^d C^d \quad (4)$$

where ϵ and δ are the parameterized entrainment and detrainment rates, respectively. Selecting C as the mixing ratio of nitrogen monoxide, [NO], Eqs. (3–4) are modified to include the internal LiNO_x production rates :

$$\frac{\partial}{\partial z}(M^u [\text{NO}]^u) = \epsilon^u \overline{[\text{NO}]} - \delta^u [\text{NO}]^u + (\bar{\rho} A) \left. \frac{\partial [\text{NO}]^u}{\partial t} \right|_{\text{LiNO}_x} \quad (5)$$

$$\frac{\partial}{\partial z}(M^d [\text{NO}]^d) = \epsilon^d \overline{[\text{NO}]} - \delta^d [\text{NO}]^d \quad (6)$$

The two terms on the right hand side of Eqs. (5 and 6) represent the subgrid scale transport of NO. Transport of NO is assumed to take place instantaneously during each model timestep. The third term is the LiNO_x term to be parameterized. For this simulation, no lightning production is allowed in the downdrafts. It is worth noting that no a-priori vertical placement of LiNO_x is necessary with this approach. Once produced inside the convective column, NO molecules are redistributed by upward and downward transport and detrained in the environment. The vertical placement of LiNO_x is a direct consequence of the redistribution by mass fluxes inside the convective scheme. This approach is different to what has been done in several global and regional models in which the vertical placement of LiNO_x was prescribed (Jourdain et al.,

2001; Meijer et al., 2001; Grewe et al., 2001; Labrador et al. 2004; Park et al., 2004; Labrador et al., 2005) based on cloud-scale modelling studies (Pickering et al. 1998).

The electrical activity in the thunderstorms is related to the vertical extension of the glaciated region where ice-ice particle rebounding collisions are efficient enough to explain the charging mechanisms (Reynolds et al., 1957; Takahashi, 1978; Saunders, 1992). A growing electrical field then results from the organization of dipolar, tripolar or even more complex charge structures at storm scale (Rust and MacGorman, 2002; Rust and Marshall, 1996; Stolzenburg, 2002; Barthe et al., 2005). The electrical field is broken down by a partial neutralization of the electrical charges. This is realized by a repetitive triggering of intra-cloud (IC) and cloud-to-ground (CG) flashes. The flashes lead to the formation of NO in the lightning channels after dissociation of air molecules at high temperature followed by a rapid cooling. According to the statistical regression formula of Price and Rind (1992), the total lightning frequency over land, f_f can be grossly estimated from mean cloud morphological parameters :

$$f_f = 3.44 \times 10^{-5} H_{ct}^{4.9} \quad (7)$$

H_{ct} is the cloud top height of the convective cells (in km).

Price and Rind (1993) proposed the following polynomial relationship between the thickness of the cold icy cloud (H_{fr} in km) and the IC/CG ratio, β :

$$\beta = 0.021 H_{fr}^4 - 0.648 H_{fr}^3 + 7.493 H_{fr}^2 - 36.54 H_{fr} + 63.09 \quad (8)$$

with $1 < \beta < 50$.

A scaling factor $c_{pr} = 0.97241 \exp(0.048203 \times \Delta \text{lat} \Delta \text{lon})$ is introduced by Price and Rind (1994) to adapt f_f to different mesh sizes in interval of latitude (Δlat) and longitude (Δlon) given in degree.

The combination of Eqs. (7–8), leads to the final expression of the LiNO_x production rates to be inserted in Eq. (5). It can be written in condensed form :

$$\left. \frac{\partial(\text{NO})^u}{\partial t} \right|_{\text{LiNO}_x} = \frac{\beta f_f}{1 + \beta} \times P(\text{IC}) + \frac{f_f}{1 + \beta} \times P(\text{CG}) \quad (9)$$

where the value of the mean production rate per CG and IC namely, $P(\text{CG}) = 6.7 \times 10^{26}$ of NO molecules, and $P(\text{IC}) = 6.7 \times 10^{25}$ of NO molecules, of Price et al. (1997) have been retained. It is worth noting that recent studies based on airborne observations and cloud scale modeling found that intracloud flashes are likely to be as effective in producing NO as cloud-to-ground flashes (DeCaria et al., 2000; Zhang et al., 2003; Fehr et al., 2004; Ridley et al., 2005). It is also important to note that the estimates for the lightning NO_x production based on Price and Rind (1992, 1994) and Price et al. (1997) are on the high end of current estimates in the literature (Labrador et al., 2005).

It is important to note that although the NO_x source vertical distribution is not specified a-priori, it is implicitly controlled by the vertical distribution of lightning flashes in the

model. The practical implementation of the LiNO_x parameterization is based on critical vertical levels defined in the deep convection scheme. IC flashes are equally distributed between the cloud top and the freezing levels. The CGs are located between the -10°C level (or the level of free sink if below) and the ground. The NO production in flashes is assumed to be proportional to air density following Goldenbaum and Dickerson (1993). Recent studies have shown that unimodal or bimodal distributions would be more realistic than uniform distributions as discussed in MacGorman and Rust (1998) and DeCaria et al. (2000, 2005). The sensitivity of LiNO_x sources to these assumptions during TROCCINOX is not covered by the present work. A 1D version of the model was run for one episode during the TOGA-COARE experiment in order to test the sensitivity of the NO_x to the vertical placement of CG and IC. The comparison shows that the altitudes of maximum NO_x in upper troposphere for were very close in the uniform and multimodal cases. The only notable difference was around the level of -15°C isotherm where the multimodal approach gives a local maximum. Although the parameterised convective scheme treats the entrainment and detrainment fluxes, the first order effect is to bring the LiNO_x up to the cloud outflow region with low sensitivity to the altitude of the source inside the convective column.

3 Experiment and meteorological situation

3.1 Experimental design

The instrumented campaign took place in February-March 2004. The investigated region was the tropical area around Bauru ($22^\circ 19' \text{S}$, $49^\circ 07' \text{E}$) in the São Paulo state of Brazil (Fig. 1). The region is located within the zone of most intense South Atlantic convergence zone (SACZ) convection (Liebmann et al., 1999; Carvalho et al., 2004). During the austral summer, it is characterized by frequent and vigorous mesoscale convective systems sometimes associated with extreme precipitation events (Nougès-Paegle and Mo, 1997; Liebmann et al., 2001; Carvalho et al., 2002; Carvalho et al., 2004). Most thunderstorms are associated with cold front convection in a mountainous terrain, although local thunderstorms and mesoscale convective systems are also present. In the region further west of the Bauru area, the thunderstorm characteristics are associated with local conditions, fronts, and the proximity of the Bolivian high (Pinto and Pinto, 2003). The southeastern Brazil is also one of the principal region in terms of lightning activity (Pinto et al., 1996, 1999a, b) with flash densities higher than $10 \text{ flashes km}^{-2} \text{ year}^{-1}$ (Pinto and Pinto, 2003; Pinto et al., 2003).

A fully instrumented research high flying aircraft (ceiling altitude of about 12 km), a Falcon 20, operated in the middle and upper troposphere. During the intense measurement campaign the aircraft operation was coordinated with

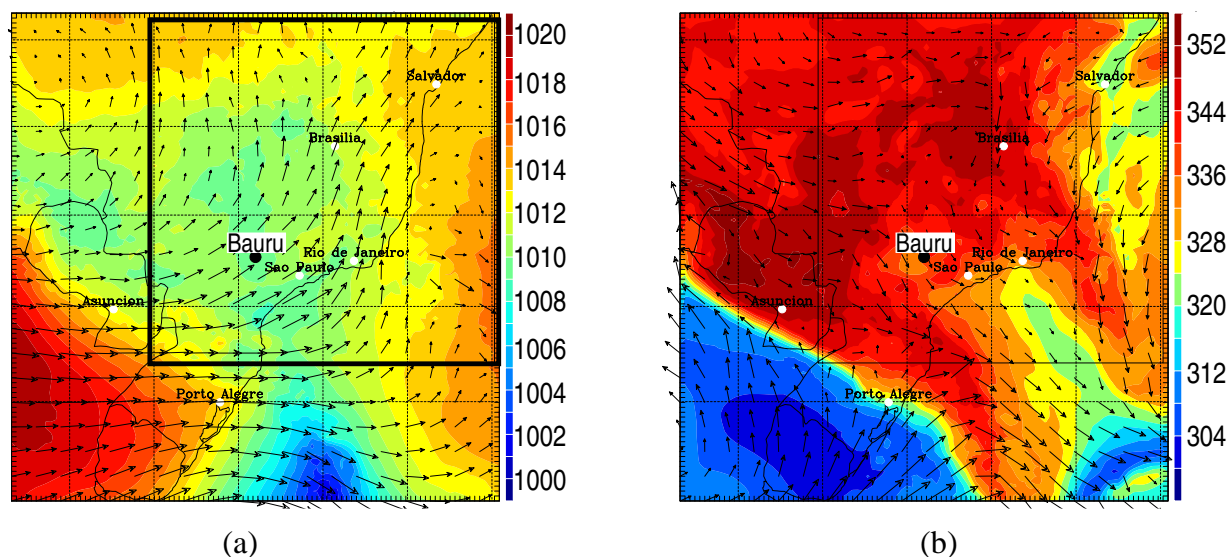


Fig. 1. Simulated meteorology on 3 March at 12:00 UTC (09:00 LT): (a) mean sea level pressure in hPa and wind vectors at the surface, (b) wet-bulb potential temperature in K and wind vectors at 850 hPa. The inside domain is used for Figs. 3, 4 and 5.

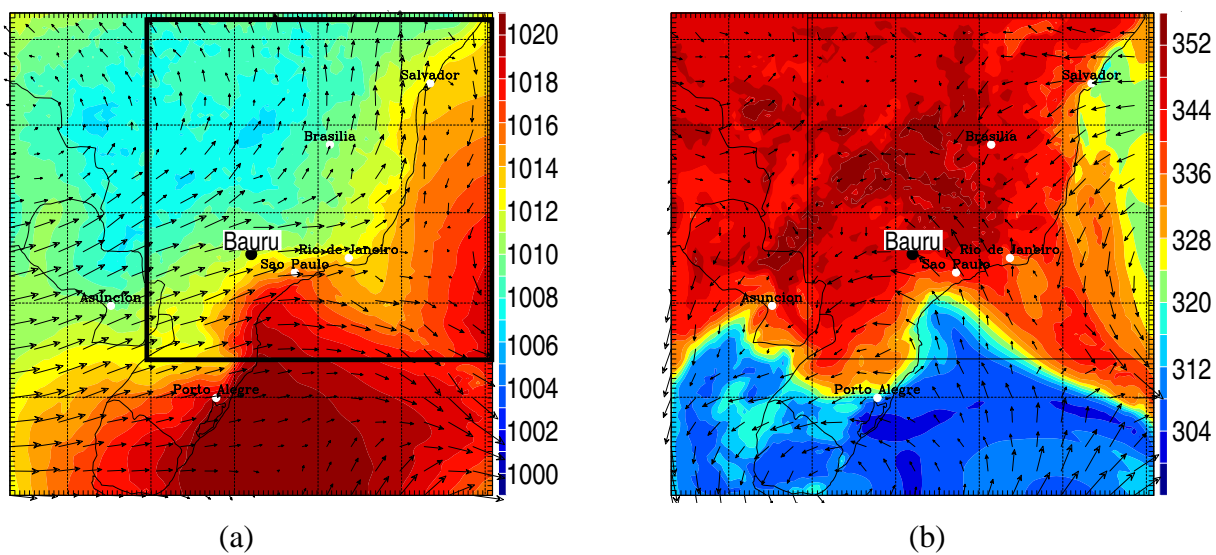


Fig. 2. Same as Fig. 1 on 4 March at 18:00 UTC (15:00 LT).

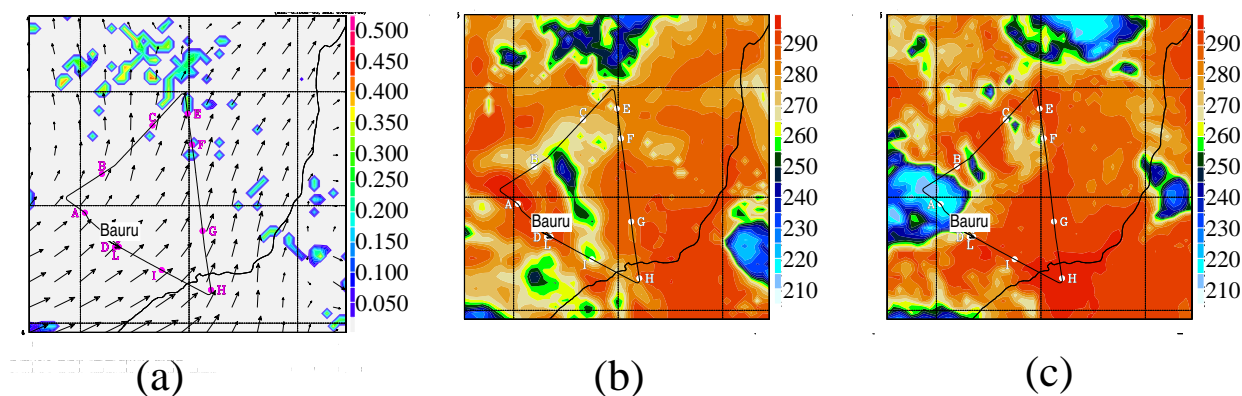


Fig. 3. (a) Simulated convective tendency for NO in pptv/s at 12 km, (b) 10.7 μm BTs (K) obtained from the Meso-NH simulation and (c) 10.7 μm BTs (K) obtained from GOES-12 observation on 3 March 2004 at 12:00 UTC. The black line displays the track of flight 9.

detailed ground-based and space borne systems (Schumann et al., overview paper in preparation). Observations in the boundary layer were also available from the Brazilian low-level aircraft although not during the dates studied here. This study focuses on three particular flights operated by the German Falcon 20 on 3–4 March. These flights were dedicated to the study of lightning NO_x with observations of both fresh and aged LiNO_x emissions. Flight 09 was a morning flight from 10:00 UTC to 14:05 UTC (07:00 LT to 11:05 LT) designed to sample the background environmental conditions, before the impact of the afternoon convective activity. Flight 10 took place in the afternoon of the same day during the peak of convective activity. The aircraft operated close to the Bauru radars and sampled outflow of fresh LiNO_x emissions. Flight 11 was devoted to the study of more aged airmasses with the objective to understand how the convection from the day before impacts the ozone budget over the region.

3.2 Mesoscale situation on 3–4 March

The SACZ is a northwest-southeast oriented quasi-stationary region of enhanced convection that extends southeastward from the ITCZ region anchored over the Amazon region into the South Atlantic Ocean. Each individual SACZ episode is composed of one or several midlatitude cold fronts that intrude into the subtropics and tropics, becoming stationary for a few days over southeastern Brazil (Carvalho et al., 2004; Liebmann et al., 1999). Figs. 1b and 2b show the southern branch of the SACZ extending partially over the southern South Atlantic. The SACZ is characterized by high values of wet-bulb potential temperature (θ_e) at 850 hPa, representative of moist and warm air masses. The position of the associated cold front is determined by the line of strong θ_e gradient along a North-West South-East axis. At 850 hPa, dry and cold air masses are simulated behind the cold front with low θ_e values (<320 K). Between 3 March and 4 March at 18:00 UTC (15:00 LT), the high pressure system moves

from the continent toward the south Atlantic, pushed north-eastward by the cold front (Fig. 1). In the free troposphere, on 3 March at 12:00 UTC (09:00 LT), the Bauru area remains under the influence of northwesterly flow with continental origin. While the front moves northeastward over the ocean on 4 March, the flow turns more southeasterly but the Bauru region remains under the influence of warm and humid airmasses. North of the cold front, the simulated upper troposphere has relatively low ozone mixing ratios, ranging from 50–60 ppbv (not show) in agreement with the observed ozone mixing ratios. On contrast, the region south of the cold front is strongly impacted by the subtropical jet stream and the subsidence below the front. In the upper and mid-troposphere, higher ozone mixing ratios (>80 ppbv) are found in the model, most probably of stratospheric origin and large-scale advection associated with the jet.

3.3 Convective activity

The convective activity that occurred during the three Falcon flights is now documented using brightness temperatures (BT) at 10.7 μm observed from GOES-12 satellite at 12:00 and 21:00 UTC 3 March and 18:00 UTC 4 March (Figs. 3, 4 and 5). In addition, the synthetic BTs calculated from the simulation are also shown. Indeed, the use of the so-called model-to-satellite approach allows us a direct comparison between simulated BT with those observed from satellite (e.g., Morcrette, 1991; Chaboureau et al., 2000; Chaboureau and Bechtold, 2005). The synthetic BT are computed using the Radiative Transfer for Tiros Operational Vertical Sounder (RTTOV) version 8.2 (Saunders et al., 2005). Observed and simulated BTs are displayed on the 30-km horizontal model grid over a sub-domain of 50 \times 50 gridpoints covering the full flight tracks.

At 12:00 UTC 3 March a deep convective cell is observed to the northwest of Bauru (point A in Fig. 3), but is missed by the simulation. Otherwise, not much convective activity

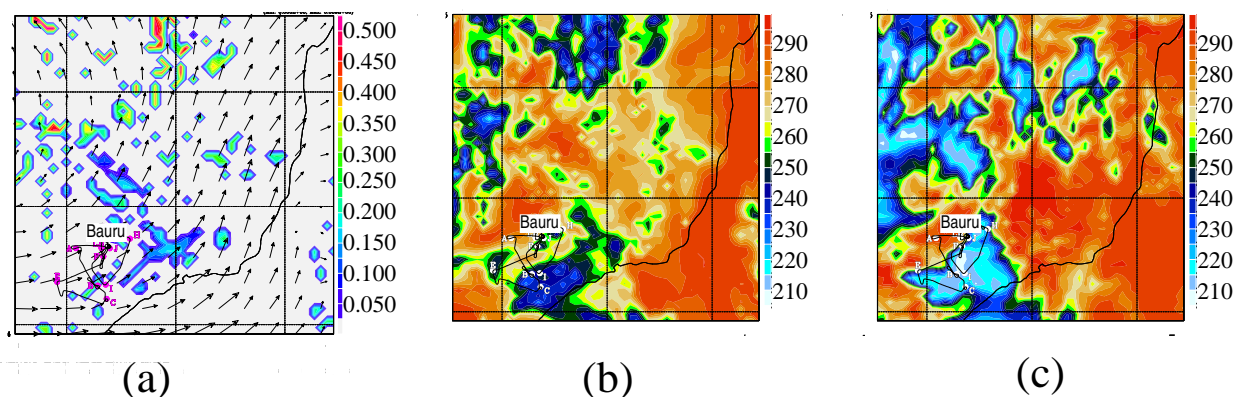


Fig. 4. Same as Fig. 3 for flight 10 on 3 March at 21:00 UTC.

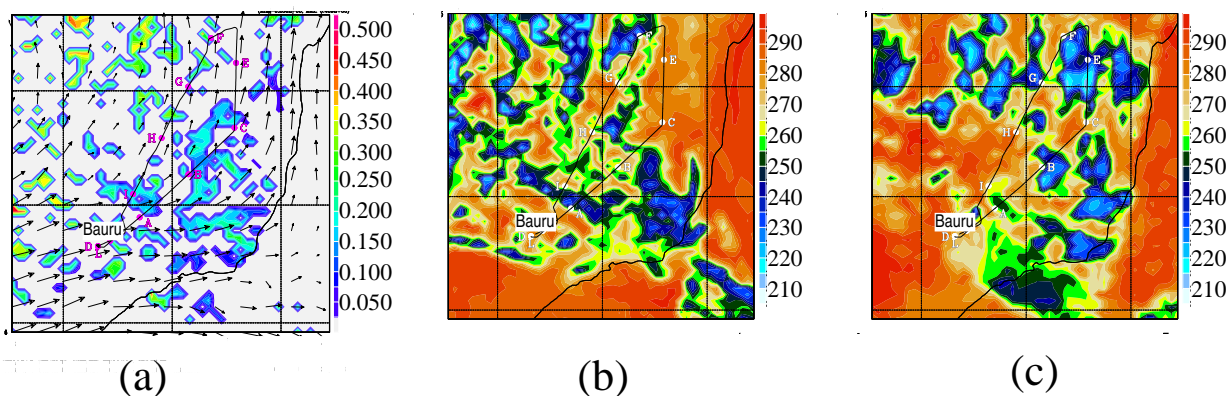


Fig. 5. Same as Fig. 3 for flight 11 on 4 March at 18:00 UTC.

and LiNO_x production are found along the track of the flight 09 in the two images showing a rather good agreement between the observation and the simulation. At 21:00 UTC 3 March, convection is well-developed over all the land part of the domain in both the observation and the simulation (Fig. 4). The convective activity is clearly associated with enhanced NO convective tendencies. The thunderstorm documented during flight 10 presents characteristics of a deep convective event with BTs less than 210 K. Lightning was also observed at 16:57 UTC by the Lightning Imaging Sensor (LIS) on board the Tropical Rainfall Measuring Mission (TRMM). The general organization of the deep convective event is well-captured by the model. However, the simulated event is located a bit too far east compared to the observation. As expected, a perfect match is not attained which makes a point-to-point comparison along the track of flight 10 difficult. At 18:00 UTC 4 March, the observed convective activity and associated NO source have moved further north (Fig. 5). The simulated BTs display a similar pattern, but with lower BTs to the west than the observed ones. The track of flight 11 encounters several convective cells in both the observation and the simulation, but not exactly at the same

locations. Overall, the simulation appears rather realistic compared to the observation, but it can miss some individual cells probed by the Falcon. This result is further shown by the time evolution of several variables over the same domain of 50×50 gridpoints (Fig. 6). The average simulated BT displays a comparable time evolution to the observed one, but with less variation from day-to-day. However, the other simulated fields present a succession of three marked diurnal cycles. The average convective available potential energy (CAPE), the total number of intracloud lightning, and the percentage of cloud tops higher than 8 km within the domain are in phase, peaking at 18:00 UTC (15:00 LT). These simulated peaks precede the observed afternoon one by about three hours, as already noted by several studies on the diurnal cycle (e.g., Chaboureaud and Bechtold, 2005, among many others).

4 Aircraft observations and model analysis

Flight 09 was designed to study the environmental conditions before the peak of convective activity. The model reproduces well the meteorological parameters (not shown) along the

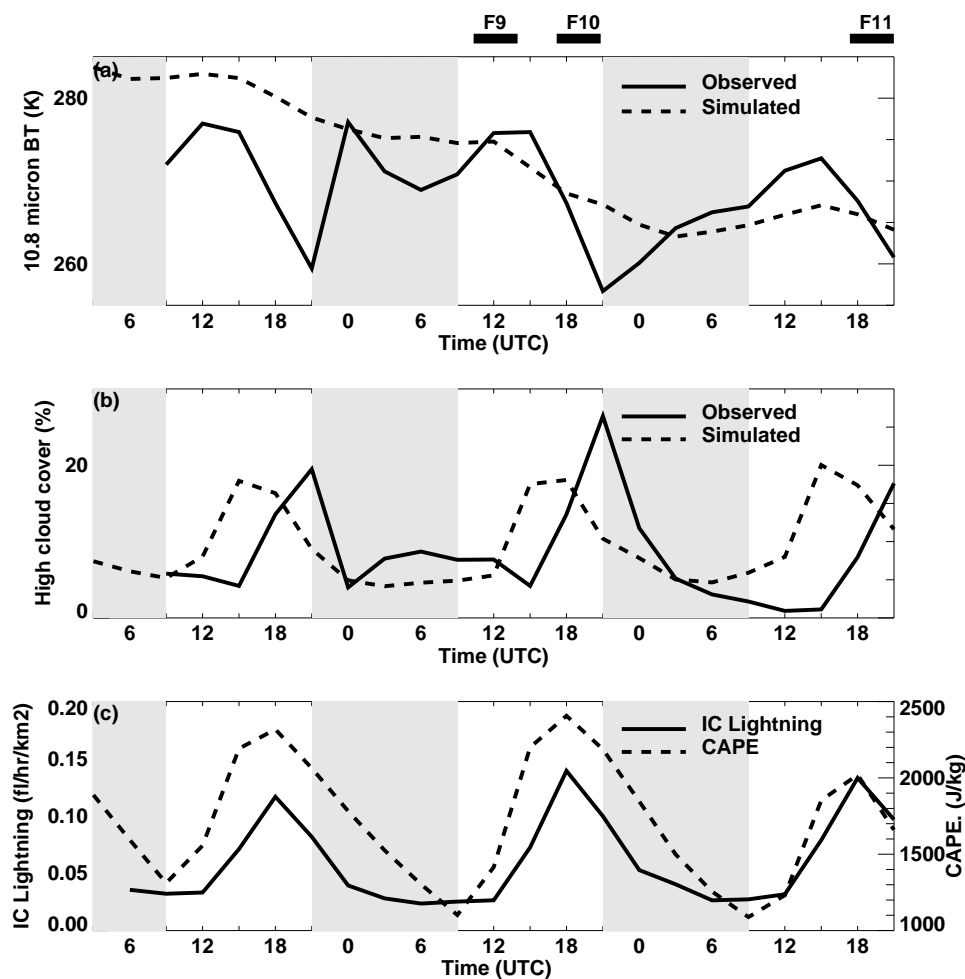


Fig. 6. Time evolution of several convective fields from 03:00 UTC 2 March till 21:00 UTC 4 March over the domain shown in Fig. 3. Grey shading indicate night periods. (top) Observed and simulated 10.7 μm averaged BTs (K). (middle) Percentage of observed and simulated high cloud cover over the domain (%). (bottom) Domain integrated number of simulated intracloud lightning ($\text{fl}/\text{h}/\text{km}^2$) and averaged convective available potential energy (J/kg^{-1}).

flight track. Fig. 7 shows the simulated and observed O₃ and NO-NO_y mixing ratios along the flight track. Two simulations were performed with and without the lightning source of NO_x. Adding the LiNO_x source significantly improves the simulation of NO and NO_y with higher mixing ratios at the levels of the Falcon flight (around 12 km) in agreement with the observations. The lightning emission of NO_x is thus the major source of NO_x and NO_y in this region. The impact of the LiNO_x source on ozone in the upper troposphere becomes significant during the second half of the flight with an increase of ozone mixing ratio by 10–15 ppbv when the LiNO_x source is triggered. During flight 09, the first maximum of NO_x mixing ratio observed by the aircraft during its ascent is well captured. According to the model and satellite images (see previous section), this maximum of NO_x originates from convection southwest of segment A-B in Fig. 3. These high NO_x mixing ratios were then advected thus corre-

sponding to sources of aged lightning NO_x. High mixing ratios are again observed and simulated while the aircraft was over the Sao Paulo region, before the final descent toward Gavião Peixoto, close to Bauru. According to the model results and the satellite images there was no convective activity over the Sao Paulo area at this time (segment G-H-I in Fig. 3). A fast vertical transport of polluted air masses from the megacity is thus unlikely. Indeed, a vertical cross-sections of NO (not shown) shows that the NO uplifted or produced by lightning in the continental convection west of the domain is transported toward the Sao Paulo region and the ocean where it mixes with clean oceanic air.

The second flight (Flight 10) was dedicated to the study of the local convection in the afternoon of the same day. The aircraft remained close to the Bauru radars and sampled fresh LiNO_x emissions. Observed NO mixing ratios reached very high values (>15 ppbv). In Fig. 8, although the model

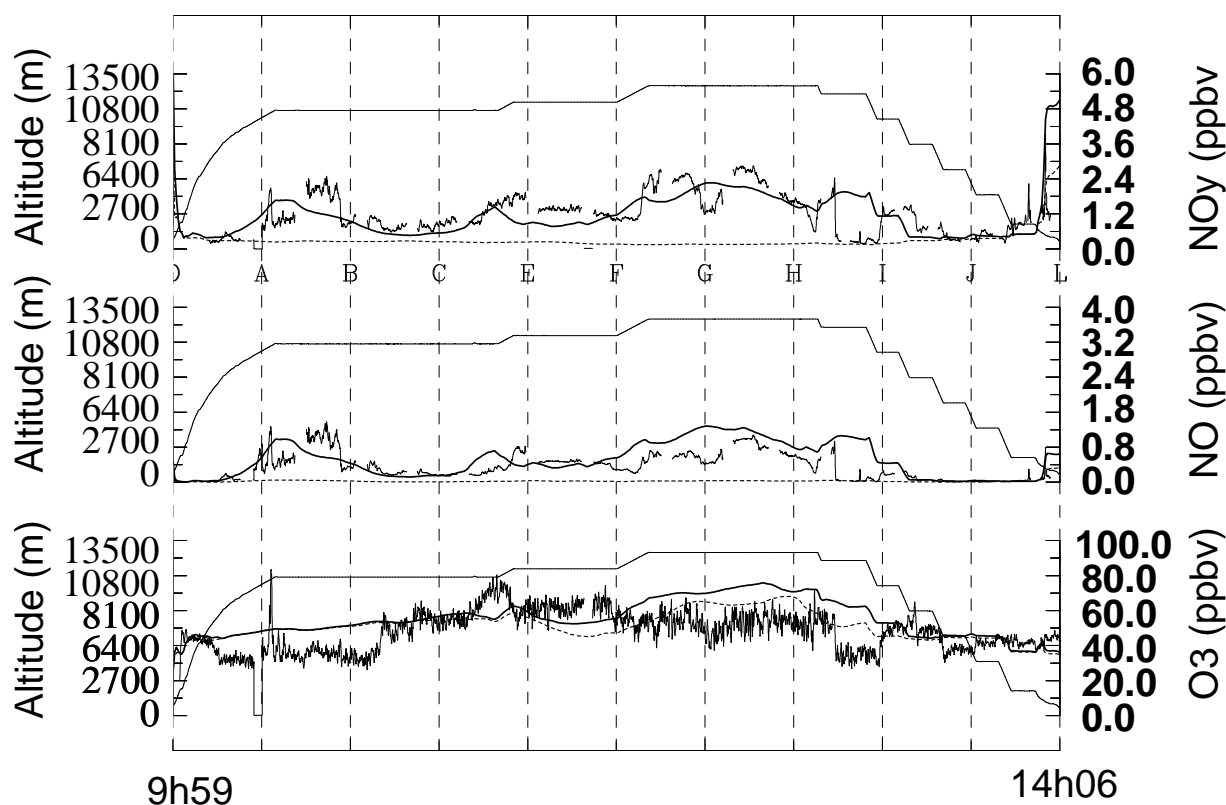


Fig. 7. Simulated and observed (thick solid line) values over the entire duration of flight 09 of (a) NO_y in ppbv, (b) NO in ppbv and (c) O₃ in ppbv. The thin solid line represents the altitude of the flight in hPa. The dotted lines represents the mixing ratios without the LiNO_x source (close to zero for NO and NO_y).

reproduces the two maxima of convection activity at the beginning and the end of the flight, it cannot capture the very high mixing ratios of NO and NO_y observed during these two periods. The reason for this underestimation is the coarse model resolution compared to the typical spatial and duration scales of the LiNO_x events. As for flight 09, the ozone mixing ratios are increased by 10 to 20 ppbv at 12 km when the LiNO_x source is active.

Flight 11 took place the day after and extended the exploration area in the upper troposphere northward up to 12° S. Observed NO and NO_y mixing ratios were lower than during the previous two flights with NO mixing ratios always less than 2 ppbv (Fig. 9). During this flight, the model tends to overestimate the observed NO and NO_y mixing ratios. This overestimation of NO_x by the model can be due to (1) overestimation of convective activity and the associated LiNO_x source or (2) missing heterogeneous sinks for nitrogen reservoirs like HNO₃. The formation of HNO₃ occurs through the direct reaction of NO₂ and OH. The destruction rate of HNO₃, however, is relatively slow with a lifetime of approximately 20 to 30 days in the tropics. Because the photochemical rate of destruction of HNO₃ is much slower than its production rate, especially in the tropics, the cycling of NO_x

through the chemical destruction of HNO₃ is slow (Brasseur et al., 1998). Since the conversion of HNO₃ to NO₂ is slow, the supposed overestimation of HNO₃ in the upper troposphere will not produce a large increase in the NO_x concentrations. The less efficient conversion of NO_x to HNO₃ in the upper troposphere allows the increase of NO_x due to lightning as has been shown by the satellite data (Zhang et al., 2000). Thus NO_x levels in the upper troposphere will be more strongly impacted by the convective activity than by recycling from HNO₃. As shown previously, the northern part of the domain was characterized by numerous convective cells, leading to an increase of lightning produced NO_x. The overestimation of NO_x by the model is certainly due mostly to the vigorous convective activity simulated during flight 11 together with a memory effect of the upper troposphere to convective activity during the previous 2 days.

5 Regional lightning NO_x budget

One important aspect of the LiNO_x budget is to characterize the vertical distribution of the LiNO_x source and subsequent transport by the updraft and downdraft in the convective

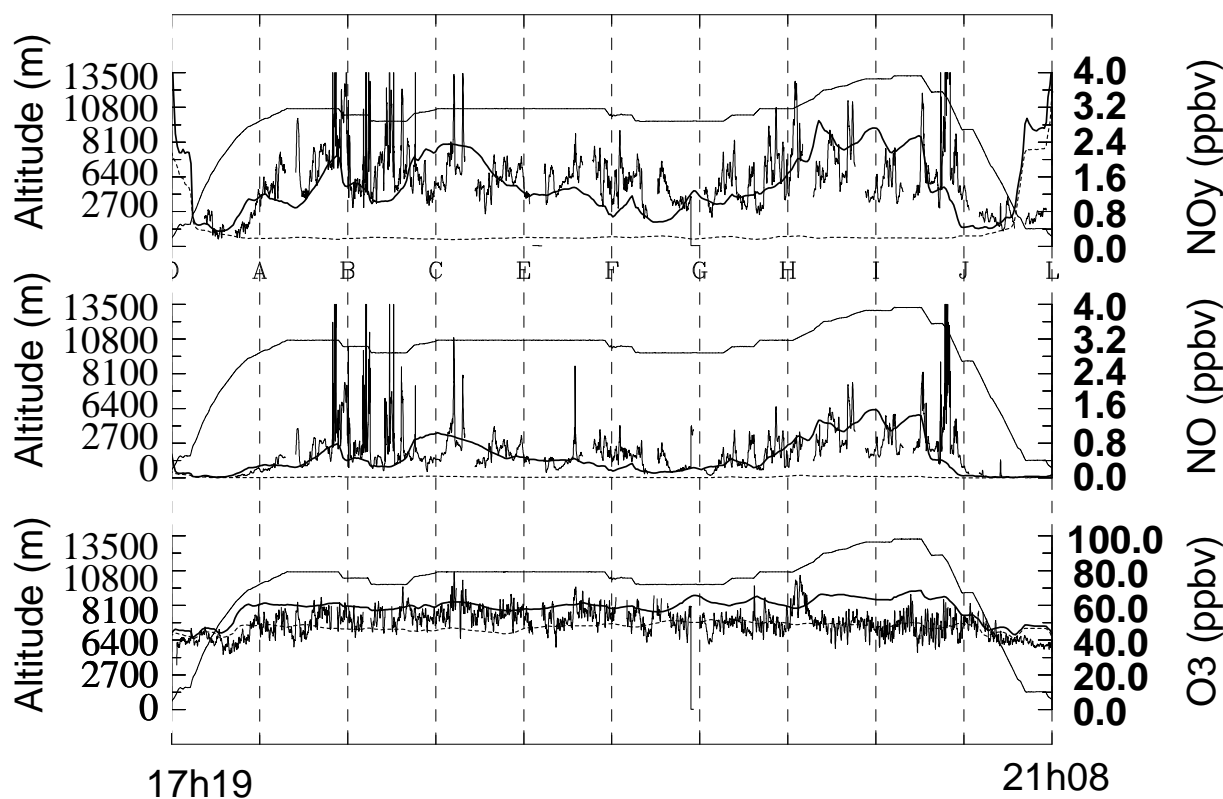


Fig. 8. Same as Fig. 7 for flight 10.

cells. In this paper, the vertical distribution of NO_x is not given a-priori but is a consequence of the diagnosed location of IC and CG flashes, entrainment of environmental air and detrainment at different levels of the clouds (see Sect. 2). The detrainment flux represents what is really gained by the troposphere. Figure 10 shows the total regional convective fluxes, in kg(N)/s/m, calculated from the model over the whole domain of simulation. Entrainment of NO into the convective cells is very low during the three days of simulation. It is interesting to note that the production of NO inside the convective cells is significant from 4 km to 16 km altitude with maxima obtained in the 5 km to 8 km altitude range. Within this layer, the maxima of NO production by lightning increases with time. Detrainment of NO to the environment starts at 4 km altitude and peaks at 12 km on 3 March at 12:00 UTC and 14–15 km during the maximum of convective activity. The maximum of NO detrained to the environment is obtained during the day of maximum regional LiNO_x production on 4 March at 18:00 UTC. From these profiles, it is clear that the NO detrained back to the environment mainly originates from lightning source inside the convective column. Only a small fraction is pumped from the boundary layer. The production of LiNO_x in kg(N)/s/m shows high values below the cloud base which are associated with the production in the CG flashes below the cloud base and to a much lesser extent to the redistribution by

downrafts of LiNO_x produced in the updrafts (no production of LiNO_x is allowed in the downrafts). There were no appropriate measurements during the studied flights to show whether or not production of NO occurred below the cloud base. This production, however, remains confined below the cloud base with very low re-entrainment into the cloud. If the regional vertical profiles of detrainment fluxes of NO are now integrated over the vertical (i.e. sum over the layer from 4 to 16 km height), the total NO production by lightning released to the troposphere ranges between 75 kg(N)/s to 400 kg(N)/s (Fig. 11). The integrated detrainment fluxes have a well pronounced diurnal cycle with peaks between 15:00 and 18:00 UTC like other convective parameters (Fig. 6). The detrainment by the downrafts is two orders of magnitude lower than the detrainment by the updrafts (in the layer from 4 to 16 km height). The count of active convective columns in the model varies from 500 (during nighttime) to 3000 (during daytime on 4 March 2004 at 18:00 UTC) which represents about 5 to 30 % of the total number of grid points in the model. This count is coherent with the percentage of observed and simulated deep convective events over the domain (Fig. 6 (middle)). The detrainment flux of NO per convective column based on the regional flux divided by the total number of active convective cells gives a production between 0.02 to 0.8 kg(N)/s/convective cell. This production per convective column is in the range of

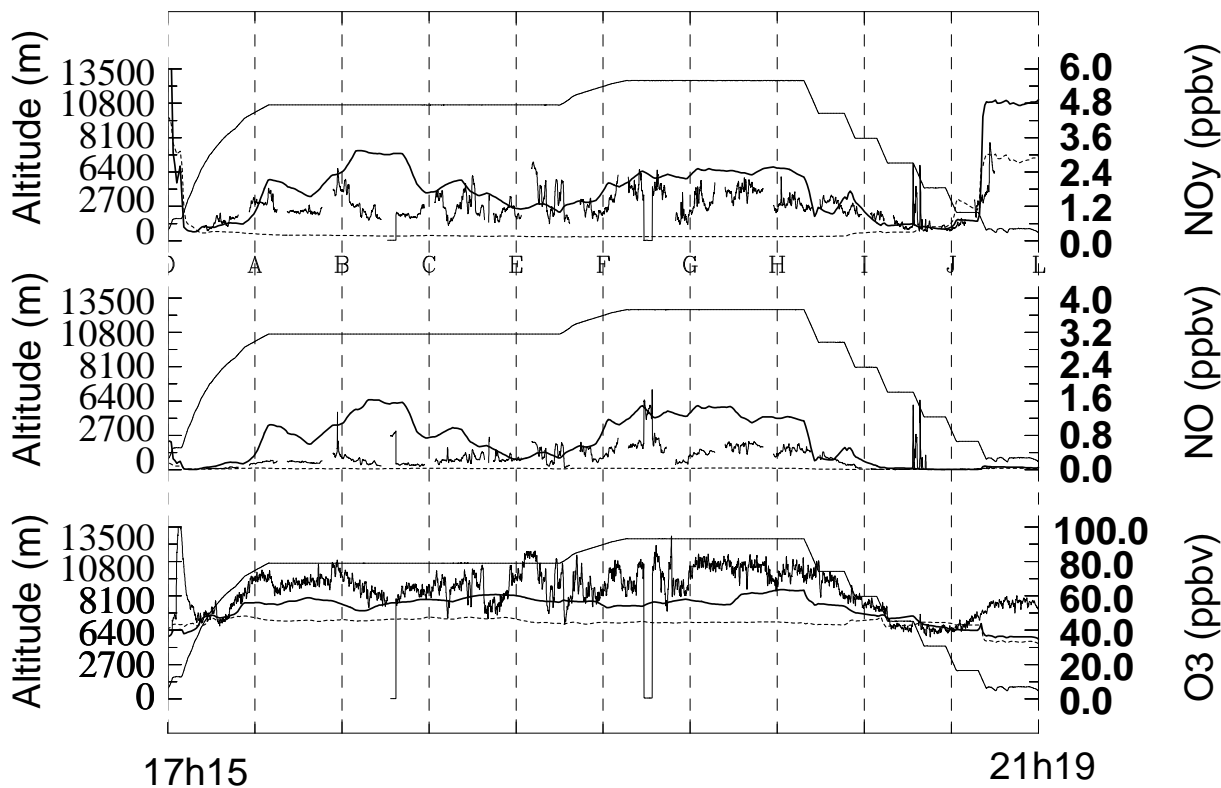


Fig. 9. Same as Fig. 7 for flight 11.

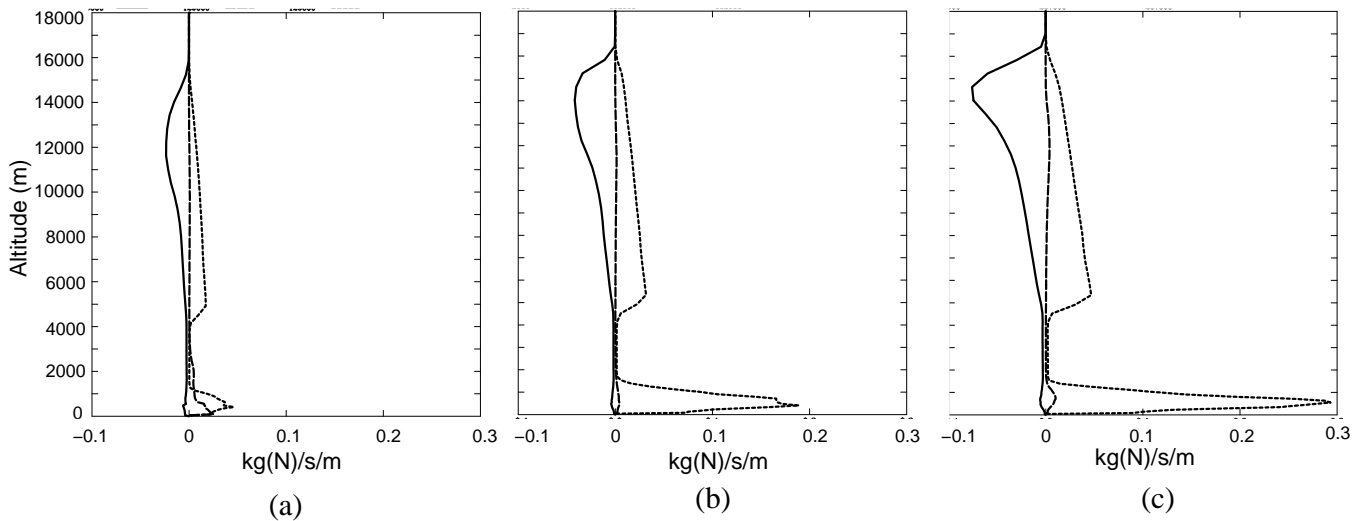


Fig. 10. Total simulated vertical profiles of convective detrainment flux (solid line), entrainment fluxes (dashed line) and lightning NO production flux (dotted line), in kg(N)/s/m at (a) 12:00 UTC (09:00 LT) on 3 March, (b) 21:00 UTC (18:00 LT) on 3 March 2004 and (c) 18:00 UTC (15:00 LT) on 4 March 2004. The fluxes are summed over the whole domain of the simulation (see Fig. 1).

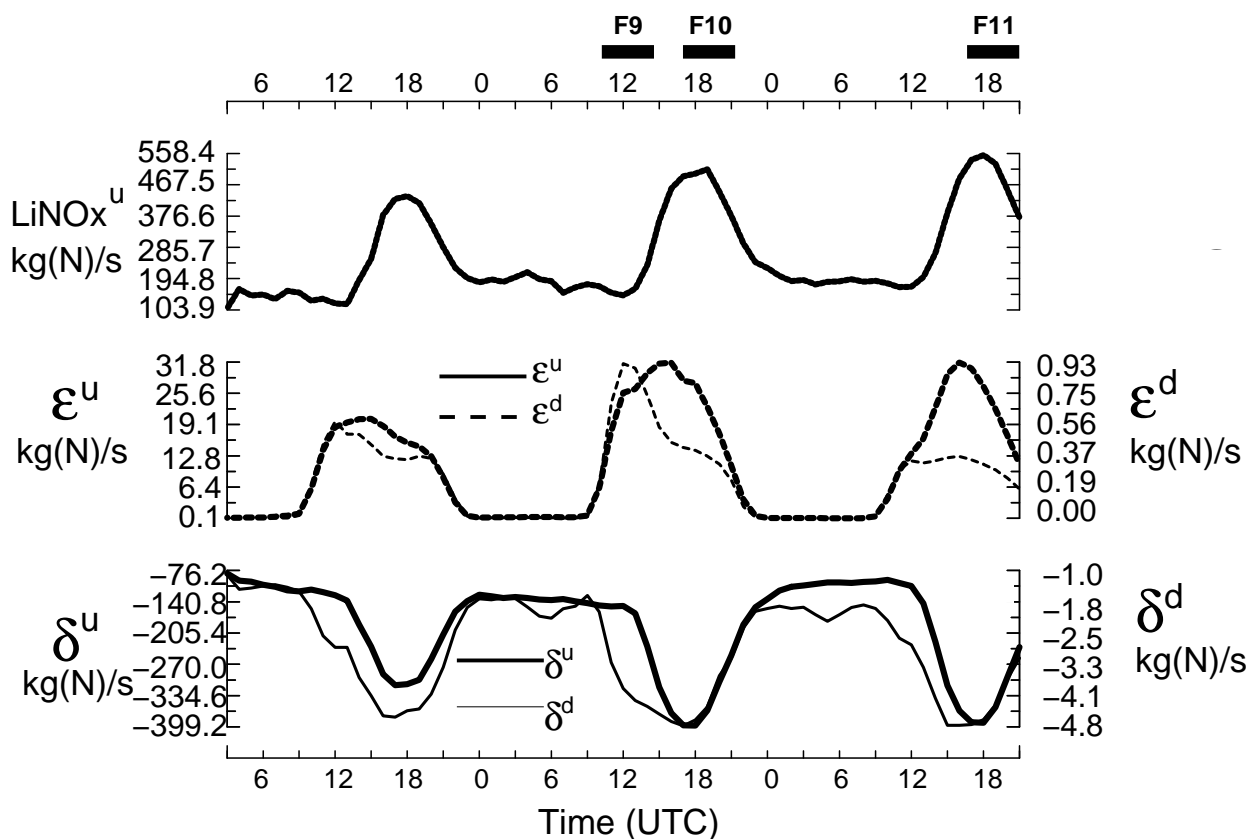


Fig. 11. Time evolution of simulated convective fluxes from 03:00 UTC 2 March till 21:00 UTC 4 March summed over the domain shown in Fig. 3, for the layer from 4 to 16 km height, in kg(N)/s. Top: NO production by lightning in the updrafts $(\overline{\rho A}) \left. \frac{\partial[\text{NO}]^u}{\partial t} \right|_{\text{LiNO}_x}$. Middle: entrainment fluxes in the updrafts $\epsilon^u[\overline{\text{NO}}]$ (thick dashed line) and the downdrafts $\epsilon^d[\overline{\text{NO}}]$ (thin dashed line). Bottom: detrainment fluxes in the updrafts $-\delta^u[\text{NO}]^u$ (thick solid line) and the downdrafts $-\delta^d[\text{NO}]^u$ (thin solid line).

the production rates deduced from NO_x storm budgets. During the STERAO campaign, Skamarock et al. (2003) derived a production of about 0.2 kg(N)/s from the observations. A production of 0.058 kg(N)/s/anvil can be deduced from the study of Huntrieser et al. (1998) based on the flux of detrained air in the anvil and aircraft observation of NO_x mixing ratios in the anvil.

An important objective when studying particular convective episodes is to quantify the contribution of the convection and associated LiNO_x source to the regional and global nitrogen budget. The extrapolation method, however, is not straightforward. From Christian et al. (2003), a rough estimate of the relative lightning activity occurring over southern America can be derived. From the annual cycle of the global flash rate, it can be estimated that lightning activity in March represents about 8% of the annual global activity (Fig. 7a of the cited paper). The total number of IC flashes, resp. CG flashes, over the simulated domain during the 66 h period is 2×10^7 , resp. 4×10^6 . The average total number of flashes (IC+CG) is equal to 101 fl/s (respectively 84 fl/s for IC and 17 fl/s for CG) which is higher than the average global annual

flash rate 44 fl/s. Such high flash rates have never been reported in the literature and the model certainly overestimates these rates. This could be partly due to the overestimation of the convective activity during the third day of the simulation or to the high sensitivity of flash rates to biases in the cloud top heights (Allen et al., 2000). No ground-based measurements were available for this region and these particular days to quantify the variability of the flash rates during the chosen episode. It is also worth noting that these particular days were not typical average days as they were chosen for their high convective activity. An average LiNO_x production of 3.4×10^7 kg(N)/day can be calculated for the domain from the simulated flash rates and the NO_x production per flash. Following the hypothesis rated above, based on the global to regional ratio of flash rates, a gross extrapolation gives a global LiNO_x production rate around 5.7 Tg(N)/year. The estimation is well within the range of current estimates (Price et al., 1997; Lee et al., 1997; Huntrieser et al., 1998). This result should not hide the uncertainties on the number of flash rates simulated by the model. This estimate is below the global production rate calculated by Skamarock et al. (2003)

when multiplying the LiNO_x production rate in the 10 July STERAO storm by the storm frequency number following Huntrieser et al. (1998). Uncertainties in the LiNO_x source are related to the vertical placement of the IC and CG flashes, the number of flashes and NO molecules produced per flash, the initial and lateral boundary NO_x profiles and transport parameterization. This work represents a first attempt to deduce a global scale LiNO_x budget from a regional scale simulation. To reduce the uncertainties, the parameterized approach has to be compared with explicit electrical schemes at cloud scale (Zhang et al., 2003; Barthe et al., 2006). Further work is needed to reconcile the different approaches and provide a proper way to extrapolate storm and regional NO_x budgets to global scale.

6 Conclusions

A lightning NO_x source has been implemented in the deep convection scheme of the Meso-NH mesoscale model. The LiNO_x scheme is written following a mass-flux formalism coherent with the transport and scavenging of gases inside the convective scheme. No a-priori vertical placement of LiNO_x is necessary with this approach. Once produced inside the convective column, NO molecules are redistributed by updrafts and downdrafts and detrained in the environment when the conditions are favorable. The model was applied to three particular flights during the TROCCINOX campaign over the tropical area around Bauru on 3–4 March 2004. These flights were dedicated to the study of lightning NO_x with observations of both fresh and aged LiNO_x emissions. The convective activity during the three flights was investigated using brightness temperatures at 10.7 μm observed from the GOES-12 satellite. The use of a model-to-satellite approach reveals that the simulation appears rather realistic compared to the observations. The model can miss some individual cells sampled by the aircraft due to the low horizontal resolution of the model compared to the scale of the cells. The diurnal cycle of the simulated brightness temperature, CAPE, number of IC lightning, NO entrainment flux are in phase, with a succession of three marked peaks at 18:00 UTC (15:00 LT). These simulated peaks precede the observed afternoon one by about three hours, as already noted by several studies on diurnal cycle. The comparison of the simulated NO_x with observations along the flight tracks show that the model reproduces well the observed NO_x levels when the LiNO_x source is applied. Exceptions are the very high levels of NO_x observed in the anvils during flight 10 and which horizontal and temporal scales can not be resolved by the model. The model tends to overestimate the NO_x levels in the upper troposphere during the last flight which could be due to high convective activity in the model. The budget of entrainment, detrainment and LiNO_x convective fluxes shows that the majority of the NO detrained to the environment comes from the lightning source inside the convective

columns. Entrainment of NO from the environment and vertical transport from the boundary layer were not significant during the episode. The troposphere is impacted by detrainment fluxes of LiNO_x from 4 km altitude to 16 km with maximum values around 14 km altitude. Detrainment fluxes vary between 75 kg(N)/s during nighttime to 400 kg(N)/s at the times of maximum convective activity. A first gross extrapolation of the regional LiNO_x source gives global LiNO_x production around 5.7 Tg(N)/year which is within the current estimates. The model however tends to overestimate the number of flash in light of global mean flash rates. Further work is still needed to reconcile the global, regional and storm approaches and provide a way to extrapolate case studies to global NO_x budget.

Acknowledgements. Computer time has been provided by the Institute du Développement et des Ressources en Informatique Scientifique (IDRIS). We thank V.-H. Peuch from Meteo-France/CNRM/GAME for providing us with the large-scale chemistry fields from the MOCAGE CTM model. This research was supported by the TROCCINOX project funded by the European Commission under the contract EVK2-CT-2001-00122. The authors thank M. Salzmann and A. DeCaria for their very constructive reviews.

Edited by: M. G. Lawrence

References

- Allen, D. J., Pickering, K., Stenchikov, G., Thompson, A., and Kondo, Y.: A three-dimensional total odd nitrogen (NO_y) simulation during SONEX using a stretched-grid chemical transport model, *J. Geophys. Res.*, 105, 3851–3876, 2000.
- Barthe, C., Molinie, G., and Pinty, J.-P.: Description and first results of an explicit electrical scheme in a 3D cloud resolving model, *Atmos. Res.*, 76, 95–113, 2005.
- Barthe, C., Pinty, J. P., and Mari, C.: Lightning-produced NO_x in an explicit electrical scheme: a STERAO case study, *J. Geophys. Res.*, in press, 2006.
- Bechtold, P., Bazile, E., Guichard, F., Mascart, P., and Richard, E.: A mass-flux convection scheme for regional and global models, *Q. J. R. Meteorol. Soc.*, 127(573), 869–886, 2001.
- Bradshaw, J., Davis, D., Grodzinsky, G., Smyth, S., Newell, R., Sandholm, S., and Liu, S.: Observed distributions of nitrogen oxides in the remote free troposphere from the NASA global tropospheric experiment programs, *Rev. Geophys.*, 38(1), 61–116, 2000.
- Brasseur, G., Muller, J.-F., and Granier, C.: Atmospheric impact of NO_x emissions by subsonic aircraft: A three-dimensional model study, *J. Geophys. Res.*, 101(D1), 1423–1428, 1996.
- Brasseur, G., Hauglustaine, D. A., Walters, S., Rasch, P. J., Muller, J.-F., Granier, C., and Tie, X. X.: MOZART, a global chemical transport model for ozone and related chemical tracers, 1, Model description, *J. Geophys. Res.*, 103(D21), 28 265–28 289, 1998.
- Brunner, D., Staehelin, J., Rogers, H. L., Kohler, M. O., Pyle, J. A., Hauglustaine, D., Jourdain, L., Bernsten, T. K., Gauss, M., Isaksen, I., Meijer, E., van Velthoven, P., Pitari, G., Mancini, E.,

- Grewe, V., and Sausen, R.: An evaluation of the performance of chemistry transport models by comparison with research aircraft observations. Part 1: concepts and overall model performance, *Atmos. Chem. Phys.*, 3, 1609–1631, 2003, <http://www.atmos-chem-phys.net/3/1609/2003/>.
- Carvalho, L. M., Jones, C., and Liebmann, B.: Extreme precipitation events in southeastern South America and large-scale convective patterns in the South Atlantic Convergence Zone, *J. Climate*, 15(17), 2377–2394, 2002.
- Carvalho, L. M., Jones, C., and Liebmann, B.: The South Atlantic Convergence Zone: Intensity, Form, Persistence and Relationships with Intraseasonal to Interannual activity and extreme rainfall, *J. Climate*, 17(1), 88–108, 2004.
- Chaboureaud, J.-P. and Bechtold, P.: Statistical representation of clouds in a regional model, and the impact on the diurnal cycle of convection during TROCCINOX *J. Geophys. Res.*, 110, D1710, doi:10.1029/2004JD005645, 2005.
- Chaboureaud, J.-P., Cammas, J.-P., Mascart, P., Pinty, J.-P., Claud, C., Roca, R., and Morcrette, J.-J.: Evaluation of a cloud system life-cycle simulated by Meso-NH during FASTEX using METEOSAT radiances and TOVS-3I cloud retrievals, *Q. J. R. Meteorol. Soc.*, 126, 1735–1750, 2000.
- Christian, H. J., Blakeslee, R. J., Boccippio, D. J., Boeck, W. L., Buechler, D. E., Driscoll, K. T., Goodman, S. J., Hall, J. M., Koshak, W. J., Mach, D. M., and Stewart, M. F.: Global frequency and distribution of lightning as observed from space by the Optical Transient Detector, *J. Geophys. Res.*, 4005, doi:10.1029/2002JD002347, 2003.
- Crassier, V., Suhre, K., Tulet, P., and Rosset, R.: Development of a reduced chemical scheme for use in mesoscale meteorological models, *Atmos. Env.*, 34(16), 2633–2644, 2000.
- Crawford, J., Davis, D., Olson, J., et al.: Evolution and chemical consequences of lightning-produced NO_x observed in the North Atlantic upper troposphere, *J. Geophys. Res.*, 105, 19 795–19 809, 2000.
- DeCaria, A. J., Pickering, K. E., Stenchikov, G. L., et al., A cloud-scale model study of lightning-generated NO_x in an individual thunderstorm during STERAO-A, *J. Geophys. Res.*, 105(D9), 11 601–11 616, 2000.
- DeCaria, A. J., Pickering, K. E., Stenchikov, G. L., and Ott, L. E.: Lightning-generated NO_x and its impact on tropospheric ozone production: A three-dimensional modeling study of a Stratosphere-Troposphere Experiment: Radiation, Aerosols and Ozone (STERAO-A) thunderstorm, *J. Geophys. Res.*, 110(D14), D14303, doi:10.1029/2004JD005556, 2005.
- Dye, J. E., Ridey, B. A., Skamarock, W., et al.: An overview of the Stratospheric-Tropospheric Experiment: Radiation, Aerosols, and Ozone (STERAO)-Deep Convection experiment with results for the July 10, 1996 storm, *J. Geophys. Res.*, 105(D8), 10 023–10 045, 2000.
- Fehr, T., Holler, H., and Huntrieser, H.: Model study on production and transport of lightning-produced NO_x in a EULINOX supercell storm, *J. Geophys. Res.*, 109(D9), D09102, doi:10.1029/2003JD003935, 2004.
- Goldenbaum G. C. and Dickerson, R. R.: Nitric oxide production by lightning discharges, *J. Geophys. Res.*, 98, 18 333–18 338, 1993.
- Grewe, V., Brunner, D., Dameris, M., Grenfell, J. L., Hein, R., Shindell, D., and Staehelin, J.: Origin and variability of upper tropospheric nitrogen oxides and ozone at northern mid-latitudes, *Atmos. Env.*, 35(20), 3421–3433, 2001.
- Hauglustaine, D., Emmons, L., Newchurch, M., et al.: On the role of lightning NO_x in the formation of tropospheric ozone plumes: A global model perspective, *J. Atmos. Chem.*, 38(3), 277–294, 2001.
- Huntrieser, H., Schlager, H., Feigl, C., et al.: Transport and production of NO_x in electrified thunderstorms: Survey of previous studies and new observations at midlatitudes, *J. Geophys. Res.*, 103(D21), 28 247–28 264, 1998.
- Huntrieser, H., Feigl, C., Schlager, H., Schroder, F., Gerbig, C., van Velthoven, P., Flato, F., Thery, C., Petzold, A., Holler, H., and Schumann, U.: Airborne measurements of NO_x, tracer species and small particles during the European Lightning Nitrogen Oxides Experiment *J. Geophys. Res.*, 107(D11), 4113, doi:10.1029/2000JD000209, 2002.
- Josse, B., Simon, P., and Peuch, V. H.: Radon global simulations with the multiscale chemistry and transport model MOCAGE, *Tellus Ser. B*, 56(4), 339–356, 2004.
- Jourdain, L. and Hauglustaine, D. A.: The global distribution of lightning NO_x simulated on-line in a general circulation model, *Phys. Chem. Earth*, 26(8), 585–591, 2001.
- Labrador, L. J., von Kuhlmann, R. and Lawrence, M. G.: Strong sensitivity of the global mean OH concentration and the tropospheric oxidizing efficiency to the source of NO_x from lightning *Geophys. Res. Lett.*, 31(6), L06102, doi:10.1029/2003GL019229, 2004.
- Labrador L. J., von Kuhlmann, R., and Lawrence, M. G.: The effects of lightning-produced NO_x and its vertical distribution on atmospheric chemistry: sensitivity simulations with MATCH-MPIC, *Atmos. Chem. Phys.*, 5, 1815–1834, 2005, <http://www.atmos-chem-phys.net/5/1815/2005/>.
- Lafore, J. P., Stein, J., Asencio, N., et al.: The Meso-NH Atmospheric simulation system, I. Adiabatic formulation and control simulations, *Ann. Geophys.*, 16, 90–109, 1994, <http://www.ann-geophys.net/16/90/1994/>.
- Lamarque, J.-F., Brasseur, G., Hess, P., and Muller, J.-F.: Three-dimensional study of the reactive contributions of the different nitrogen sources in the troposphere, *J. Geophys. Res.*, 102(D9), 10 873–10 873, 1997.
- Lee, D. S., Köhler, I., Grobler, E., Rohrer, F., Sausen, R., Gallardo-Klenner, L., Olivier, J. G. J., Dentener, F. J., and Bouwman, A. F.: Estimations of Global NO_x emissions and their uncertainties, *Atmos. Env.*, 31, 1735–1749, 1997.
- Liebmann, B., Kiladis, G. N., Marengo, J. A., Ambrizzi, T., and Glick, J. D.: Submonthly convective variability over the South America and the South Atlantic convergence zone, *J. Climate*, 12(7), 1877–1891, 1999.
- Liebmann, B., Jones, C., and de Carvalho, L. M. V.: Interannual variability of daily extreme precipitation events in the state of São Paulo, Brazil, *J. Climate*, 14(2), 208–218, 2001.
- MacGorman, D. R. and Rust, W. D.: The electrical nature of storms, Oxford, pp422, 1998.
- Mari, C., Jacob, D. J., and Bechtold, P.: Transport and scavenging of soluble gases in a deep convective cloud, *J. Geophys. Res.*, 105, 22 255–22 267, 2000.
- Martin, R. V., Jacob, D. J., Logan, J., Ziemke, J. M., and Washington, R.: Detection of a lightning influence on tropical tropospheric ozone, *Geophys. Res. Lett.*, 27, 1639–1642, 2000.
- Massart, S., Cariolle, D., and Peuch, V. H.: Towards an im-

- provement of the atmospheric ozone distribution and variability by assimilation of satellite data, *Comptes Rendus Geoscience*, 337(15), 1305–1310, 2005.
- Masson, V.: A physically-based scheme for the urban energy budget in atmospheric models, *Bound. Layer Meteorol.*, 1994, 357–397, 2000.
- Meijer, E. W., van Velthoven, P. F. L., Brunner, D., Huntrieser, H., and Kelder, H.: Improvement and evaluation of the parameterisation of nitrogen oxide production by lightning, *Phys. Chem. Earth.*, 26(8), 577–583, 2001.
- Mlawer, E. J., Taubman, S. J., Brown, P. D., Iacono, M. J., and Clough, S. A.: Radiative transfer for inhomogeneous atmospheres: RRTM, a validated correlated-k model for the long-wave, *J. Geophys. Res.*, 102D, 16 663–16 682, 1997.
- Morcrette, J.-J.: Radiation and cloud radiative properties in the European centre for medium range weather forecasts forecasting system, *J. Geophys. Res.*, 96, 9121–9132, 1991.
- Noilhan, J.: A simple parameterization of land surface processes for meteorological models, *Mon. Wea. Rev.*, 117, 536, 1989.
- Nougés-Paegle, J. and Mo, K. C.: Alternating wet and dry conditions over South America during summer, *Mon. Wea. Rev.*, 125(2), 279–291, 1997.
- Olivier, J. G. J. and Berdowski, J. J. M.: Global emissions sources and sinks. in: “The Climate System”, Berdowski, J., edited by: Guicherit, R. and Heij, B. J., 33–78. A.A. Balkema Publishers/Swets and Zeitlinger Publishers, Lisse, The Netherlands, 2001a.
- Olivier, J. G. J., Berdowski, J. J. M., Peters, J. A. H. W., Bakker, J., Visschedijk, A. J. H., and Bloos, J.-P. J.: Applications of EDGAR. Including a description of EDGAR 3.0: reference database with trend data for 1970–1995. RIVM, Bilthoven. RIVM report no. 773301 001/ NOP report no. 410200 051, 2001b.
- Park, M., Randel, W. J., Kinnison, D. E., Garcia, R. R., and Choi, W.: Seasonal variation of methane, water vapor, and nitrogen oxides near the tropopause: Satellite observations and model simulations, *J. Geophys. Res.*, 109(D3), D03302, doi:10.1029/2003JD003706, 2004.
- Pickering, K. E., Wang, Y. S., Tao, W. K., Price, C., and Muller, J. F.: Vertical distributions of lightning NO_x for use in regional and global chemical transport models, *J. Geophys. Res.*, 103(D23), 31 203–31 216, 1998.
- Pinto, O., Gin. R. B. B., Pinto, I. R. C. A., Mendes, O., Diniz, J. H., Carvalho, A. M.: Cloud-to-ground lightning flash characteristics in southeastern Brazil for the 1992–1993 summer season, *J. Geophys. Res.*, 101(D23), 29 627–29 635, 1996.
- Pinto, O., Pinto, I. R. C. A., Gomes, M. A. S. S., Vitorello, I., Padilha, A. L., Diniz, J. H., Carvalho, A. M., and Cazetta Filho, A.: Cloud-to-ground lightning in southeastern Brazil in 1993 1. Geographical distribution, *J. Geophys. Res.*, 104(D24), 31 369–31 379, 1999a.
- Pinto, I. R. C. A., Pinto, O., Rocha R. M. L., Diniz, J. H., Carvalho, A. M., and Cazetta Filho, A.: Cloud-to-ground lightning in southeastern Brazil in 1993: 2. Time variations and flash characteristics, *J. Geophys. Res.*, 104(D24), 31 381–31 387, 1999b.
- Pinto, I. R. C. A. and Pinto, O.: Cloud-to-ground lightning distribution in Brazil, *J. Atmos. Solar-Terr. Phys.*, 65(6), 733–737, 2003.
- Pinto, O., Pinto, I. R. C. A., Diniz, J. H., Fihlo, A. C., Cherchiglia, L. C. L., and Carvalho, A. M.: A seven-year study about the negative cloud-to-ground lightning flash characteristics in Southeastern Brazil, *J. Atmos. Solar-Terr. Phys.*, 65(6), 739–748, 2003.
- Price, C., and Rind, D.: A simple lightning parameterization for calculating global lightning distributions, *J. Geophys. Res.*, 97, 9919–9933, 1992.
- Price, C. and Rind, D.: What determines the cloud-to-ground lightning fraction in thunderstorms?, *Geophys. Res. Lett.*, 20, 463–466, 1993.
- Price, C., and Rind, D.: Modeling global lightning distributions in a General Circulation Model, *Mon. Wea. Rev.*, 122, 1930–1939, 1994.
- Price, C., Penner, J., and Prather, M.: NO_x From Lightning, Part I: Global Distribution Based on Lightning Physics, *J. Geophys. Res.*, 102, 5929–5941, 1997.
- Ridley B. A., Pickering, K. E., and Dye, J. E.: Comments on the parameterization of lightning-produced NO in global chemistry-transport models, *Atmos. Env.*, 39, 6184–6187, 2005.
- Reynolds, S. E., Brooks, M., and Gourley, M. F.: Thunderstorm charge separation, *J. Meteorol.*, 14, 426–436, 1957.
- Rust W. D. and Marshall, T. C.: On abandoning the thunderstorm tripole-charge paradigm *J. Geophys. Res.*, 101, 23 499–23 500, 1996.
- Rust W. D. and MacGorman, D. R.: Possibly inverted-polarity electrical structures in thunderstorms during STEPS, *Geophys. Res. Lett.*, 29(12), doi:10.1029/2001GL014303, 2002.
- Saunders, C. P. R.: A review of thunderstorm electrification processes, *J. Appl. Meteorol.*, 32, 642–655, 1992.
- Saunders, R., Brunel, P., English, S., Bauer, P., O’Keeffe, U., Francis, P., and Rayer, P.: RTTOV-8 Science and validation report. NWP SAF Report, 41 pages, 2005.
- Skamarock, W. C., Powers, J., Barth, M. C., Dye, J., Matejka, T., Bartels, D., Baumann, K., Stith, J. L., Parrish, D., and Hubler, G.: Numerical simulations of the 10 July STERAO/Deep convection experiment convective system: Kinematics and transport, *J. Geophys. Res.*, 105, 19 973–19 990, 2000.
- Stolzenburg, M., Marshall, T. C., Rust, W. D., and Bartels, D. L.: Two simultaneous charge structures in thunderstorm convection, *J. Geophys. Res.*, 107, 4352, doi:10.1029/2001JD000904, 2002.
- Skamarock, W. C., Dye, J. E., Defer, E., Barth, M. C., Stith, J. L., Ridley, B. A., and Baumann, K.: Observational- and modeling-based budget of lightning-produced NO_x in a continental thunderstorm, *J. Geophys. Res.*, 108(D10), 4305, doi:10.1029/2002JD002163, 2003.
- Takahashi, T.: Riming electrification as a charge generation mechanism in thunderstorms, *J. Atmos. Sci.*, 35, 1536–1548, 1978.
- Tie, X. X., Zhang, R. Y., Brasseur, G., Emmons, L., and Lei, W.: Effects of lightning on reactive nitrogen and nitrogen reservoir species in the troposphere, *J. Geophys. Res.*, 106(D3), 3167–3178, 2001.
- Zhang, R., Sanger, N. T., Orville, R. E., Tie, X. X., Randel, W., and Williams, E. R.: Enhanced NO_x by lightning in the upper troposphere and lower stratosphere inferred from the UARS global NO₂ measurements, *Geophys. Res. Lett.*, 27, 685–688, 2000.
- Zhang, X. J., Helsen, J. H., and Farley, R. D.: Numerical modeling of lightning-produced NO_x using an explicit lightning scheme: 1. Two-dimensional simulation as a “proof of concept”, *J. Geophys. Res.*, 108(D18), A1–A20, 2003.